Dielectric and optical properties of pure liquids by means of *ab initio* reaction field theory

Yi Luo,[1] Patrick Norman,[2] Hans Ågren,[2] Kristian O. Sylvester-Hvid,[3] and Kurt V. Mikkelsen[1]
[1]*Department of Chemistry, University of Copenhagen, DK-2100 Copenhagen Ø, Denmark*
[2]*Department of Physics and Measurement Technology, Linköping University, S-581 83 Linköping, Sweden*
[3]*Department of Chemistry, Aarhus University, DK-8000 Århus C, Denmark*
(Received 2 June 1997; revised manuscript received 23 December 1997)

A general Onsager-type reaction field theory approach for simulating dielectric and optical properties is proposed, thereby giving a unified description for both macroscopic and microscopic properties of pure liquids. A demonstration is given for *ab initio* computations of the refractive index, the density fluctuation of the refractive index, and the local field factors of benzene and acetonitrile in the liquid phase, showing good agreement with available experimental data. [S1063-651X(98)06904-9]

PACS number(s): 41.20.Bt

I. INTRODUCTION

In order to understand the microscopic origin of material bulk properties, it is necessary to interpret them in terms of molecular properties. Within the framework of a solvent continuum model, the macroscopic and microscopic properties are connected through the concept of local fields [1], which is based on the fact that individual molecules are not polarized by the external Maxwell electric field but by a local field that is a superposition of the Maxwell field and the field produced by the surrounding medium. Using a spherical cavity model, Onsager [2] and Böttcher [1,3] divided the local field into a cavity field, depending only on the solvent dielectric constant, and a reaction field, depending on the cavity radius and the solute molecular properties. The choice of cavity radius has so far been somewhat arbitrary; the most commonly used is based on the Onsager approximation, which relates the cavity radius to the solvent density.

The solute molecular properties can be calculated at the quantum level using various self-consistent reaction field models [4–13] employing different cavity shapes—spherical [4–9,11,12], ellipsoidal [4,10], or a more irregular shape defined by a set of overlapping spherical atoms having the appropriate van der Waals radii [13]. Irrespective of cavity shape, the models so far have all involved one or more cavity size parameters, determined on the grounds of physical intuition, and different choices for the cavity radius can therefore be found in the literature. Recently, we have presented a method based on the combined use of the classical continuum approach and modern quantum chemistry reaction field theory, for determining the Onsager spherical cavity radius of pure liquids [14]. This method provides a unique value for the radius of the cavity for each electronic structure model. In this paper, we show that this method not only enables an accurate determination of the solute molecular properties but also lets us determine the local fields, and thereby the macroscopic properties of pure liquids at one and the same theoretical level. As a demonstration, calculations of the refractive index, density fluctuation of the refractive index, and local field factors of liquid benzene and acetonitrile are presented.

II. THE CLASSICAL CONTINUUM APPROACH

The classical continuum approach describes the dependence of the macroscopic properties of a dense medium on molecular quantities, such as the dipole moment μ and the polarizability α. This theory is well established as described, for instance, in the books by Böttcher [1,15]. In this section, we will only recapitulate the necessary elements for introducing the properties of interest.

A. Static properties

According to Böttcher [1], a general connection between macroscopic quantities, in terms of the dielectric constant, and microscopic quantities, in terms of molecular properties of the pure liquid in a continuum model, should be given as

$$\frac{(\epsilon^0-1)(2\epsilon^0+1)}{3\epsilon^0}=\frac{4\pi N}{1-f_0(a)\alpha_0}\left(\alpha_0+\frac{1}{3kT}\frac{\mu^2}{1-f_0(a)\alpha_0}\right). \tag{1}$$

Here N denotes the number of particles per unit volume that can be computed from $N=dN_A/M$, where M is the molecular weight of the substance, d the density, and N_A Avogadro's number. Further, ϵ^0 is the static dielectric constant, α_0 is averaged static molecular polarizability, μ is the dipole moment of the molecule, T is the temperature, and k is the Boltzmann constant. The static reaction field factor f_0 is defined as [1]

$$f_0(a)=\frac{1}{a^3}\frac{2(\epsilon^0-1)}{2\epsilon^0+1} \tag{2}$$

in the dipole approximation, introducing the cavity radius a.

For nonpolar dielectrics, the dipole moment μ is zero, therefore, Eq. (1) reduces to the so-called Onsager-Böttcher expression

$$\frac{(\epsilon^0-1)(2\epsilon^0+1)}{3\epsilon^0}=\frac{4\pi N\alpha_0}{1-f_0(a)\alpha_0}. \tag{3}$$

It can be seen that the value chosen for the cavity radius a, which is unknown up to this point, influences the results through the reaction field factor. Using the Onsager approximation for the cavity radius

$$\frac{4\pi}{3}Na^3=1, \tag{4}$$

Eq. (3) reduces to the Clausius-Mossotti formula

$$\frac{\epsilon^0-1}{\epsilon^0+2}=\frac{4\pi}{3}N\alpha_0. \tag{5}$$

Based on the expression used for the total polarization [1], we can introduce the static local field factor l_0 as

$$l_0=\frac{3\epsilon^0}{2\epsilon^0+1}\frac{1}{1-f_0\alpha_0}\left(\alpha_0+\frac{\mu^2}{3kT}\frac{1}{1-f_0\alpha_0}\right)\Bigg/\left(\alpha_0+\frac{\mu^2}{3kT}\right). \tag{6}$$

B. Dynamic properties

In this paper we focus on properties of pure liquids in the optical region, in which case the permanent dipoles of the polar systems can no longer follow the changes of the field. The contributions from orientational polarization, i.e., the directing field, is therefore negligible. With the Maxwell relation connecting the dielectric constant and the refractive index, $\epsilon=n^2$, one obtains [cf. Eq. (3)] a relation that implicitly determines the optical refractive index n_ω,

$$\frac{(n_\omega^2-1)(2n_\omega^2+1)}{3n_\omega^2}=\frac{4\pi N\alpha(\omega)}{1-f_\omega(a)\alpha(\omega)}, \tag{7}$$

where

$$f_\omega(a)=\frac{1}{a^3}\frac{2(\epsilon^\omega-1)}{2\epsilon^\omega+1}. \tag{8}$$

This equation can be used for all liquids. If the Onsager cavity radius is used, Eq. (7) reduces to

$$\frac{n_\omega^2-1}{n_\omega^2+2}=\frac{4\pi}{3}N\alpha(\omega), \tag{9}$$

i.e., the well-known Lorenz-Lorentz equation.

Analogous to the static case, the Maxwell-to-molecular field relations can be expressed in an effective manner with the introduction of an optical local field factor l_ω, which is obtained from Eq. (6) by omitting the dipole moment. The dynamic local field factor then becomes

$$l_\omega=\frac{3\epsilon^\omega}{2\epsilon^\omega+1}\frac{1}{1-f_\omega\alpha_\omega}. \tag{10}$$

Finally, concerning the dynamic quantities we also give the expression for the density fluctuation of the refractive index ($\mathrm{d}n_\omega^2/\mathrm{d}d$) or DFRI, which is an important experimental observable. From Eq. (7) and the expression for the number of particles per unit volume, a general formula for $\mathrm{d}n_\omega^2/\mathrm{d}d$ can be obtained,

$$\frac{\mathrm{d}n_\omega^2}{\mathrm{d}d}=\frac{1}{d}\frac{n_\omega^2(n_\omega^2-1)(2n_\omega^2+1)}{2n_\omega^4+1-\frac{2}{3}(n_\omega^2-1)^2/v}, \tag{11}$$

where $v=\frac{4}{3}\pi Na^3$ represents the fraction of the volume occupied by the molecules [15]. It is interesting to note that the values of $\mathrm{d}n_\omega^2/\mathrm{d}d$ deduced from the Lorenz-Lorentz equation (9) are found to be in disagreement with experimental results [16]. The expression based on this equation becomes

$$\frac{\mathrm{d}n_\omega^2}{\mathrm{d}d}=\frac{n_\omega^2-1}{d}\frac{n_\omega^2+2}{3}. \tag{12}$$

The present approach will be compared with the Lorenz-Lorentz treatment in Sec. IV.

The procedure outlined above can be implemented for nonspherical cavities if, instead of using the average dipole moment and polarizability, the influence of different components of the dipole moment (vector) and the polarizability α (tensor) is considered. For an ellipsoidal cavity in a nonpolar solvent, this would mean that the lengths of the three axes x, y, z are to be determined from the diagonal tensor components α_{xx}, α_{yy}, α_{zz} in the same way as the spherical cavity radius is given through calculations of the average α.

III. COMPUTATIONAL PROCEDURES

As indicated in the preceding sections, accurate calculations of molecular properties are essential for the determination of macroscopic properties of dense media. Currently, self-consistent reaction field theory is most commonly used for this purpose. The solute molecular properties are then obtained through different methods such as the sum-over-state approach [7,8], the analytic derivative approach [4], or the response theory approach [5,6,13]. Response theory is of particular interest here since it provides not only static but also dynamic properties; see, for example, Refs. [7,8,4–6,13].

In general one obtains the quantities

$$\mu=R_\mu(\epsilon,a), \tag{13}$$

$$\alpha=R_\alpha(\epsilon,a), \tag{14}$$

from reaction field electronic structure calculations, i.e., with parametric dependences on the dielectric constant ϵ and the cavity radius a. The dielectric constant ϵ is naturally obtained from experiment, whereas the cavity radius cannot be uniquely chosen. In fact, there are three different commonly employed approaches for determining the cavity radius in the literature; (i) from the density of the pure liquid [2]; (ii) taking the molecular radius plus the van der Waals radii of the outermost atoms; (iii) adding a constant term (0.5 Å) to the value obtained from model (i) [17,7]. In this paper, we make use of the recently proposed method to determine a unique value for the cavity radius [14].

A. Solvation model

The utilized solvent model is a generalization of Kirkwood's model [23,24] utilizing a multipolar expansion of the solute charge distribution. The dielectric interaction energy given here is as in Refs. [24,25]

$$E_{\mathrm{sol}}=\sum_{lm} R^{lm}\langle T_{lm}\rangle, \tag{15}$$

using real spherical harmonics, and where

$$R^{lm}=g_l(\epsilon)\langle T_{lm}\rangle \tag{16}$$

and ϵ is the dielectric constant. The $\langle T_{lm}\rangle$ elements are the charge moments of the solute charge distribution and they are given as expectation values of the nuclear, T^n_{lm}, and electronic solvent operators, T^e_{lm},

$$\langle T_{lm}\rangle = T^n_{lm}-\langle T^e_{lm}\rangle. \tag{17}$$

The function $g_l(\epsilon)$, representing the response of the dielectric medium, is given by [24,25]

$$g_l(\epsilon)=-\frac{1}{2}a^{-(2l+1)}[(l+1)(\epsilon-1)]/[l+\epsilon(l+1)]. \tag{18}$$

The free energy functional for the solvated molecule is given as

$$F(\lambda)=E_{\mathrm{vac}}(\lambda)+E_{\mathrm{sol}}(\lambda), \tag{19}$$

and depends on a set of parameters $\{\lambda\}$ for the electronic wave function. The expectation value of the vacuum Hamiltonian H_{vac} is given as

$$E_{\mathrm{vac}}(\lambda)=\frac{\langle O|H_{\mathrm{vac}}|O\rangle}{\langle O|O\rangle}, \tag{20}$$

where the electronic wave function $|O\rangle$ depends on the parameter set $\{\lambda\}$.

The free-energy functional is variationally optimized with respect to the parameters of the electronic wave function. We utilize a direct, restricted-step, second order algorithm for the optimization of the energy and electronic wave function [24,25]. The parameter set $\{\lambda\}$ comprises orbital rotation parameters in the case of a single determinant reference state, or orbital rotation parameters and determinant coefficients in the case of a multideterminant reference state, as, for instance, given by the CAS and RAS wave functions described in Sec. IV A. The optimized wave function of the solute is used in the solvent response method for obtaining molecular properties of solvated molecules. This method thus appends a solvent reaction field Hamiltonian to the unperturbed solute Hamiltonian before the response of the applied time-dependent electromagnetic field is evaluated. Detailed descriptions and applications of this method can be found in Refs. [5,6]. The dipole moments are obtained as expectation values, while the polarizability is obtained as a first order response property.

B. Vibrational polarizability

The vibrational polarizability plays an important role in determining the cavity radius, and eventually all properties. The vibrational polarizability of polyatomic molecules can be calculated by introducing different approximations [18]. In this paper, the double harmonic approximation will be used for dynamic vibrational polarizability, which gives

$$\alpha^v_{ij}(-\omega;\omega)=\sum_b \left(\frac{\partial\mu^e_i}{\partial Q_b}\right)\left(\frac{\partial\mu^e_j}{\partial Q_b}\right)\Big/(\omega_b^2-\omega^2), \tag{21}$$

where ω_b is the vibrational frequency and Q_b is the normal mode coordinate associated with the normal mode b. Furthermore, average polarizabilities are computed as

$$\alpha=\frac{1}{3}(\alpha_{xx}+\alpha_{yy}+\alpha_{zz}) \tag{22}$$

for both electronic and vibrational polarizabilities.

C. Cavity radius

The cavity radius a_0 can be determined as a zero point of the deviation function $F^1(\epsilon^0,a)$, which then merely expresses the equivalence in Eq. (1) together with the reaction field expressions for the dipole moment and the polarizability in Eqs. (13) and (14); see Ref. [14],

$$F^1(\epsilon^0,a)=\frac{(\epsilon^0-1)(2\epsilon^0+1)}{3\epsilon^0}-\frac{4\pi N}{1-f_0(a)R_{\alpha_0}(\epsilon^0,a)}\times\left(R_{\alpha_0}(\epsilon^0,a)+\frac{1}{3kT}\frac{R^2_\mu(\epsilon^0,a)}{1-f_0(a)R_{\alpha_0}(\epsilon^0,a)}\right). \tag{23}$$

The motivation for this particular choice of cavity radius is that the classical continuum approach and the self-consistent reaction field should give the same physical description for any investigated system. It has been shown that a unique solution exists for the cavity radius and that this value then depends only on the molecular system and the computational level at hand [14]. The dipole moment and static polarizability of the solvated molecule are then given by $R_\mu(\epsilon^0,a_0)$ and $R_\alpha(\epsilon^0,a_0)$, respectively.

D. Refractive index, local field factors, and density variation

For a given cavity radius a_0, we can introduce a second deviation function $F^2(\tilde{n}_\omega,a_0)$ by combining Eqs. (7) together with Eqs. (13) and (14),

$$F^2(\tilde{n}_\omega,a_0)=\frac{(\tilde{n}^{\,2}_\omega-1)(2\tilde{n}^{\,2}_\omega+1)}{3\tilde{n}^{\,2}_\omega}-\frac{4\pi NR_{\alpha(\omega)}(\tilde{n}_\omega,a_0)}{1-f_\omega(a_0)R_{\alpha(\omega)}(\tilde{n}_\omega,a_0)}. \tag{24}$$

Hence, the proper refractive index, which we denote by n_ω, is found at the zero point of the deviation function

TABLE I. Static polarizability of gas phase benzene. All values are in a.u.

	$b0$	$b1$	$b2$	Expt.
α^e_{xx}	75.601	78.286	79.081	79.16[a]
α^e_{zz}	36.985	43.723	44.978	44.13[a]
α^e	62.729	66.765	67.713	67.48[a]
α^v_{xx}	0.357	0.290	0.283	
α^v_{zz}	6.846	5.531	5.798	
α^v	2.520	2.037	2.121	
α_{xx}	75.958	78.576	79.364	83.54[b]
α_{zz}	43.831	49.254	50.776	43.05[b]
α	65.249	68.802	69.835	70.05[b]

[a]Rayleigh scattering depolarization ratios [27].
[b]Static Kerr effect, includes vibrational contribution [28].

$F^2(\tilde{n}_\omega, a_0)=0$. The dynamic polarizabilities of the solute molecule are then given by $R_{\alpha(\omega)}(n_\omega, a_0)$.

Knowing the consistent molecular properties, $R_\mu(\epsilon^0, a_0)$, $R_\alpha(\epsilon^0, a_0)$, and the refractive index n_ω, the local field factors, both static and dynamic, and the density fluctuation of the refractive index can be computed directly via Eqs. (6), (10), and (11).

IV. SAMPLE CALCULATIONS

We consider the pure liquids benzene ($\epsilon=2.28$) and acetonitrile ($\epsilon=37.5$) to represent samples of nonpolar and strong polar dielectrics, and choose them as test cases for the proposed method.

A. Computational details

For the benzene molecule three different basis sets, denoted as $b0$, $b1$, and $b2$, have been employed. Basis sets $b0$ and $b1$ are built from a standard 4-31G basis set [19] and the atomic natural orbital (ANO) basis set (C[$14s9p4d/4s3p1d$], H[$8s4p/2s1p$]) [20], respectively, by supplementing diffuse $p(0.05)$ and $d(0.05)$ functions on carbon, and the third basis set $b2$ is from Sadlej's polarization basis sets [21]. The molecule is placed in the xy plane. All calculations are carried out using the random phase approximation (RPA) linear response method [linear response applied to a single determinant reference state, also equivalent to the time-dependent Hartree-Fock (TDHF) method].

The acetonitrile molecule possesses C_{3v} symmetry, and has here been represented by placing the main symmetry axis along the z axis. All results are obtained with Sadlej's polarization basis sets [21]. However, for reasons explained below, we have, in addition to the SCF reference state, also employed a limited complete active space (CAS) with four electrons in two doubly degenerate orbitals, denoted as $2e$ and $3e$ (4 in 4). These orbitals originate mainly from degenerate p_x and p_y atomic orbitals (AO) localized on the neighboring carbon and nitrogen atoms, thereby forming (degenerate) bonding and antibonding C-N molecular orbitals (MO). The $1e$ MO, on the other hand, is mainly localized to the other carbon atom, and it is kept inactive together with the other seven occupied a_1 orbitals. Furthermore, an extensive, full valence, restricted active space (RAS) has been

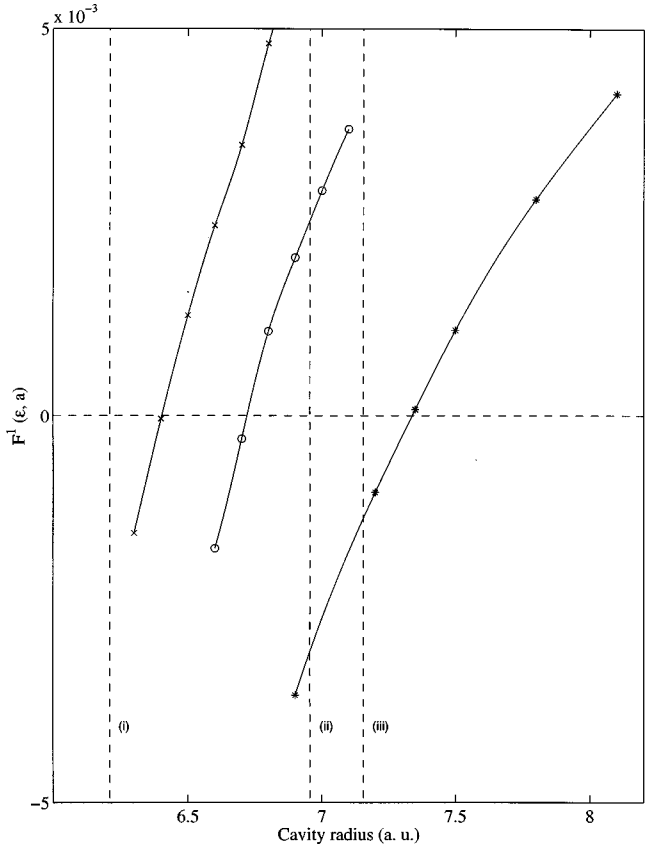

FIG. 1. Deviation functions $F^1(\epsilon^0, a)$ versus cavity radius a for liquid benzene with different basis sets. The true cavity radius a_0 is given by $F^1(\epsilon^0, a_0)=0$. The three commonly used cavity radii, (i)–(iii) (explained in the text), are indicated by dashed lines. The three curves shown are corresponding to the cases: using basis set $b0$, only electronic contributions (dashed line with marks ''x''); using basis set $b0$, total electronic and vibrational contributions (solid line with marks ''o''); using basis set $b1$, total electronic and vibrational contributions (solid line with marks ''*'').

employed with sixteen electrons distributed in RAS1: $4a_1$, $5a_1$, $6a_1$, $7a_1$, and $1e$; RAS2: $2e$ and $3e$; and RAS3: $8a_1$, $9a_1$, $10a_1$, $11a_1$, and $4e$ (16 in 16). The number of electrons in RAS1 is kept between ten to twelve and in RAS3 between zero to two, whereas no restrictions are imposed on RAS2. The active spaces are motivated by the clear separation in MP2 occupation numbers that exist between the four orbitals in RAS2 (the same four orbitals as in the CAS) and others. Furthermore, only the three core orbitals ($1a_1$, $2a_1$, and $3a_1$) are kept inactive in the RAS, and the valence orbitals in RAS1 are balanced by equally many unoccupied orbitals in RAS3, thereby correlating all orbitals with MP2 occupation numbers greater than 10^{-2}.

The molecular properties in the gas phase have been calculated without inclusion of the reaction field, since the interactions among molecules are very small in the gas phase. All calculations are performed with the DALTON quantum chemistry program package [22].

B. Nonpolar dielectrics: Liquid benzene

The RPA averaged static polarizability of benzene with basis set $b2$ is found to be in excellent agreement with experiment, cf. Table I. The results with basis set $b1$ are

TABLE II. Frequency dependent vibrational polarizabilities of benzene in gas phase and solution. All values are in a.u.

ω	$b0$		$b1$	
	α_{gas}	α_{liq}	α_{gas}	α_{liq}
0.00	2.520	3.015	2.037	2.315
0.01	−0.376	−0.524	−0.250	−0.307
0.02	−0.218	−0.231	−0.175	−0.192
0.03	−0.076	−0.083	−0.060	−0.067
0.04	−0.041	−0.045	−0.032	−0.035
0.05	−0.025	−0.028	−0.020	−0.022
0.06	−0.017	−0.019	−0.014	−0.015
0.07	−0.013	−0.014	−0.010	−0.011
0.08	−0.010	−0.011	−0.008	−0.008
0.09	−0.008	−0.009	−0.006	−0.007
0.10	−0.006	−0.007	−0.005	−0.005

slightly below, whereas $b0$ is apparently too small to provide accurate values. Hence, with an adequate basis set the polarizability of benzene can be well described at the RPA level and correlated methods are not expected to improve results in the present work.

The deviation functions $F^1(\epsilon^0,a)$ obtained with basis sets $b0$ and $b1$ at the RPA level are shown in Fig. 1. The vibrational contribution to the polarizability of liquid benzene, $\alpha=R_\alpha(\epsilon,a)$, has also been included. The values for the cavity radius a_0 are strongly basis set dependent, as shown in the previous study [14]. Also the inclusion of the pure vibrational contribution to the polarizability was found to have a significant effect on the cavity radius, e.g., with basis set $b0$, cavity radii of 6.401 and 6.753 (a.u.) were obtained by excluding and including the pure vibrational contributions, respectively.

With the proper cavity radius, one is thus able to compute the refractive index. In the optical region, it is understandable that the vibrational contribution is small due to the short interaction time. In Table II, the frequency dependent vibrational polarizabilities of benzene are summarized for both the gas and liquid phases. The solvent results are obtained with the cavity radius a_0. In the static limit, the vibrational

TABLE III. Refractive indices of liquid benzene.

ω	Basis	This work	LL[a]			Expt.
			(i)	(ii)	(iii)	
0.0430	$b0$	1.492	1.538	1.503	1.497	1.4825[b]
	$b1$	1.494	1.584	1.545	1.538	
0.0770	$b0$	1.512	1.559	1.522	1.515	1.4979[c]
	$b1$	1.515	1.609	1.566	1.559	
0.0908	$b0$	1.523	1.572	1.533	1.526	1.5075[c]
	$b1$	1.525	1.624	1.579	1.571	
0.1050	$b0$	1.537	1.588	1.547	1.540	1.5196[c]
	$b1$	1.537	1.643	1.595	1.587	

[a]The solvated molecular properties are calculated by using the three commonly used cavity radii, (i)–(iii).
[b]Experimental value quoted in Ref. [29].
[c]Experimental values quoted in Ref. [30].

TABLE IV. Density fluctuation of the refractive indices and local field factors for liquid benzene.

	Density fluctuation						
			LL			Local field factor	
ω	This work	Case 1[e]	Case 2[f]	Case 3[g]	Expt.[d]	This work	LL[c]
0.000						1.379[a]	1.425
						1.343[b]	
0.0430	1.677[a]	1.910	2.267[a]	1.883[a]		1.370[a]	1.399
	1.655[b]		2.588[b]	2.050[b]		1.332[b]	
0.0770	1.761[a]	2.007	2.410[a]	1.980[a]		1.385[a]	1.415
	1.732[b]		2.773[b]	2.165[b]		1.352[b]	
0.0834	1.784[a]	2.039	2.445[a]	2.003[a]	1.80	1.388[a]	1.419
	1.758[b]		2.818[b]	2.192[b]		1.355[b]	
0.0908	1.815[a]	2.068	2.502[a]	2.040[a]		1.393[a]	1.424
	1.776[b]		2.888[b]	2.234[b]		1.358[b]	
0.1050	1.879[a]	2.146	2.617[a]	2.116[a]		1.407[a]	1.436
	1.837[b]		3.037[b]	2.323[b]		1.366[b]	

[a]Basis set $b0$.
[b]Basis set $b1$.
[c]Using experimental values of refractive indices.
[d]Experimental values quoted in Ref. [15].
[e]LL formula, Eq. (12), with experimental values of refractive indices.
[f]LL formula, Eq. (12), with the calculated refractive indices using cavity radii (i).
[g]LL type of general expression for DFRI, where $v=1$ is assumed in Eq. (11), and the calculated refractive index using cavity radius (i).

TABLE V. Dipole moments and gas phase polarizabilities for the acetonitrile molecule. Theoretical polarizabilities are purely electronic. Dynamic values at 514.5 nm. All values are in a.u.

	Static			Dynamic			
	SCF	CAS	RAS	SCF	CAS	RAS	Expt.[a]
μ_z	1.67	1.53	1.52	1.67	1.53	1.52	1.54
α_{zz}	38.52	36.44	36.84	39.80	37.57	38.01	40.7
α_{xx}	23.95	23.59	23.48	24.54	24.16	24.05	25.3
α	28.81	27.87	27.93	29.62	28.63	28.70	30.4
dispersion				2.8%	2.7%	2.8%	

[a]Experimental values from Ref. [27].

polarizability for liquid benzene is strongly enhanced compared to gas phase values. Increases of 20% and 14% are observed for basis sets $b0$ and $b1$, respectively. Compared to the static value, the dynamic vibrational polarizability in the optical region decreases drastically. Furthermore, the difference between values in gas and liquid phases becomes negligible for larger frequencies. In general, the vibrational contribution to the dynamic polarizability in the optical region can be neglected.

With Eq. (24), the refractive index of liquid benzene at different frequencies has been obtained, see Table III. Basis sets $b0$ and $b1$ have been used for the simulation. It can be seen from Table III that the calculated refractive indices of liquid benzene seem to be very stable with respect to the basis set. The agreement with experimental data is most satisfactory and we can report theoretical estimations within 1%. For comparison, we have also applied the widely used Lorenz-Lorentz (LL) equation [Eq. (9)] for alternative values of the refractive index. The frequency dependent polarizabilities are then computed at three commonly used cavity radii (i), (ii), and (iii). All results are summarized in Table III and we note the strong basis set dependence that can be seen, the same as that found in Ref. [26]. In fact, the better basis set provides poorer results in comparison with experimental data. For instance, at cavity radius (i), the error increases from 4% to 8% with the two different basis sets. In addition, the results also show strong dependence on the cavity radius. We recall that the LL equation is derived under the assumption that the cavity radius is determined by the density of the medium, see Eq. (4). Therefore, only the choice of cavity radius (i) is consistent with the LL equation, and since this is a poor choice as shown in Fig. 1 the deficiency is not surprising.

The density fluctuation of the refractive index (DFRI) at different frequencies has been calculated by applying Eq. (11) for both basis sets. The results obtained from the LL-type formula with experimental data for the refractive index have also been included for comparison. As shown in Table IV, the values obtained from the current model are in excellent agreement with the experimental data, whereas the result from the LL-type formula overshoots by 13%. We have further examined the validity of the LL-type formula by using the calculated refractive indices from the LL model, Eq. (9), where α is obtained from basis set $b0$ and $b1$ at cavity radius (i). The DFRI results, listed in Table IV as case 2, overshoot the experimental value by 36% and 57% for basis sets $b0$ and $b1$, respectively. It is interesting to see that if one assumes $v=1$ in Eq. (11), another LL-type formula can be obtained. Using this formula with the calculated refractive index from the LL model, the DFRI data are found to be larger than the experimental one by 11% and 22% for basis sets $b0$ and $b1$, respectively, see case 3 in Table IV.

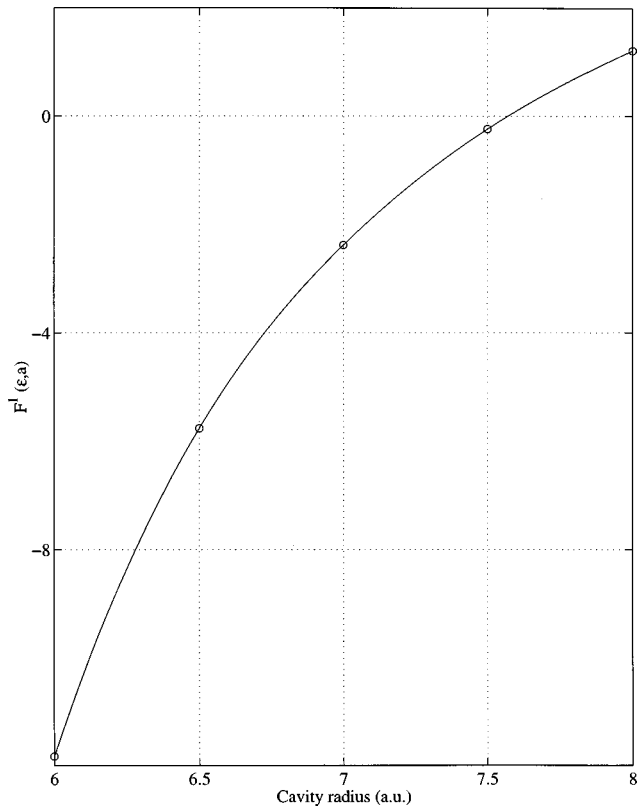

FIG. 2. Deviation function $F^1(\epsilon^0,a)$ versus cavity radius a in atomic units for acetonitrile with $\epsilon^0=37.5$. For comparison, the van der Waals based cavity radius is 6.085 atomic units, and the liquid density (0.786 g cm^{-3}) based cavity radius is 5.103 atomic units.

The static and dynamic local field factors from our model are found to be rather close to those obtained from the LL approximation, as shown in Table IV. However, for polar dielectrics, the difference between the present model and the LL formalism for local field factors will become larger, especially the static values. This will be further demonstrated in the next section.

C. Polar dielectrics: Liquid acetonitrile

As a model medium for the group of polar dielectrics, we have chosen acetonitrile with a static dielectric constant of

TABLE VI. Frequency dependent vibrational polarizabilities for acetonitrile in gas and liquid phase. All values are in a.u.

ω	α^v_{gas}	α^v_{liq}
0.00	0.264	0.403
0.02	−0.028	−0.030
0.04	−0.005	−0.006
0.06	−0.002	−0.003
0.08	−0.001	−0.002
0.10	−0.001	−0.001

TABLE VII. Refractive index, density fluctuation, and local field factor for liquid acetonitrile.

	Refractive index		Density fluctuation			Local field factor	
ω	This work	Expt.	This work	LL	Expt.	This work	LL
0.0000						1.701	1.91
0.0770	1.320	1.3416[b]	1.067	1.296	1.12[a]	1.191	1.267
0.0937	1.324	1.3456[b]	1.083	1.317		1.195	1.270
0.1049	1.327	1.3490[b]	1.095	1.335		1.198	1.273

[a]Experimental values quoted from Ref. [16].
[b]Experimental values quoted from Ref. [30].

37.5. The cavity radius of polar dielectrics is strongly dependent on the molecular properties, especially on the dipole moment. At the SCF level the calculated dipole moment (1.67 a.u.) significantly overestimates the experimental value of 1.54 a.u. Already with the relatively small, and only statically correlated, CAS reference state the correct dipole moment is obtained, and a further extension to the full valence correlated RAS reference state shows that for the properties of interest CAS basically covers the full correlation effect, cf. Table V. Therefore, only the CAS reference state will be used for calculations of liquid acetonitrile. A consistent cavity radius of 7.55 a.u. is obtained with the aid of Eq. (23) by incorporating the pure vibrational contribution to the average polarizability according to Eq. (21). The deviation function $F^1(\epsilon^0,a)$ is plotted in Figure 2 for cavity radii in the range of 6.0–8.0 a.u. The cavity radius, corresponding to the zero point crossing, is much larger than cavity radii previously used in the literature based on liquid density ($a=5.103$ a.u.) and van der Waals radii ($a=6.085$ a.u.).

With the proper cavity radius at hand, we turn to the determination of the optical refractive index through Eq. (24). As seen from Table VI, the vibrational contribution to the polarizability α^v is negligible at optical frequencies and has therefore been neglected. However, conforming with the results for benzene, we note that the solvent effect on α^v, being large in the static limit (53%), decreases drastically for nonzero frequencies. In Table VII, we present the consistent refractive indices and compare them with experimental data where such are available. The theoretical values are within 2%, which is comparable to the accuracy found for benzene.

Results for the DFRI in liquid acetonitrile at several frequencies are given in Table VII. The result calculated from the present model at $\omega=0.043$ a.u. underestimates the experimental value by 6%. However, this is still a considerable improvement compared to the LL value, which overshoots by 17%, cf. Table VII. The LL value was obtained by using experimental refractive index.

Finally, we present in Table VII also the local field factors that relate the external Maxwell field and the molecular field. Accurate local field factors are a prerequisite for a comparison between hyperpolarizability measurements in the liquid phase and theoretical models. For acetonitrile two values have been used in the literature [4] based on the LL approximation, 1.27 for the static field and 1.91 in the optical region. A reinvestigation of the electric field induced second harmonic generation (ESHG) experiment on acetonitrile with improved local field factors will follow in a later publication. In this context the differences are expected to be crucial since the measurement involves the combination of one static and three optical fields, thereby yielding a total field factor of $l_0 l_\omega^2 l_{2\omega}$.

ACKNOWLEDGMENTS

Y. Luo greatly appreciates the financial support provided by the Hellmuth Hertz Foundation. This work was supported by the Danish and Swedish Natural Science Research Councils.

[1] C. J. F. Böttcher, *Theory of Electric Polarization, Vol. I* (Elsevier, Amsterdam, 1973), pp. 166–178.
[2] L. Onsager, J. Am. Chem. Soc. **58**, 1486 (1936).
[3] C. J. F. Böttcher, Physica (Amsterdam) **9**, 945 (1942).
[4] A. Willetts and J. E. Rice, J. Chem. Phys. **99**, 426 (1993).
[5] K. V. Mikkelsen, P. Jørgensen, and H. J. Aa. Jensen, J. Chem. Phys. **100**, 6597 (1994).
[6] K. V. Mikkelsen, Y. Luo, H. Ågren, and P. Jørgensen, J. Chem. Phys. **100**, 8240 (1994).
[7] S. Di Bella, T. J. Marks, and M. A. Ratner, J. Am. Chem. Soc. **116**, 4440 (1994).
[8] J. Yu and M. C. Zerner, J. Chem. Phys. **100**, 7487 (1994).
[9] K. V. Mikkelsen, Y. Luo, H. Ågren, and P. Jørgensen, J. Chem. Phys. **102**, 9362 (1995).
[10] C. Dehu, F. Meyers, E. Hendrickx, K. Clays, A. Persoons, S. R. Marder, and J. Brédas, J. Am. Chem. Soc. **117**, 10 127 (1995).
[11] Y. Luo, A. Cesar, and H. Ågren, Chem. Phys. Lett. **252**, 389 (1996).
[12] I. D. L. Albert, T. J. Marks, and M. A. Ratner, J. Phys. Chem. **100**, 9714 (1996).
[13] R. Cammi, M. Cossi, B. Mennucci, and J. Tomasi, J. Chem. Phys. **105**, 10 556 (1996).
[14] Y. Luo, H. Ågren, and K. V. Mikkelsen, Chem. Phys. Lett. **275**, 145 (1997).
[15] C. J. F. Böttcher and P. Bordewijk, *Theory of Electric Polarization, Vol. II* (Elsevier, Amsterdam, 1978), p. 293.
[16] A. Proutiere, E. Megnassan, and H. Hucteau, J. Phys. Chem. **96**, 3485 (1992).

[17] M. W. Wong, M. J. Frisch, and K. B. Wiberg, J. Am. Chem. Soc. **113**, 4776 (1991).
[18] D. M. Bishop and B. Kirtman, J. Chem. Phys. **95**, 2646 (1991).
[19] R. Ditchfield, W. J. Hehre, and J. A. Pople, J. Chem. Phys. **54**, 724 (1971).
[20] P.-O. Widmark, P. Å. Malmquist, and B. O. Roos, Theor. Chim. Acta **77**, 291 (1990).
[21] A. J. Sadlej, Theor. Chim. Acta **79**, 123 (1991).
[22] T. Helgaker, H. J. Aa. Jensen, P. Jørgensen, J. Olsen, K. Ruud, H. Ågren, T. Andersen, K. L. Bak, V. Bakken, O. Christiansen, P. Dahle, E. K. Dalskov, T. Enevoldsen, H. Heiberg, H. Hettema, D. Jonsson, S. Kirpekar, R. Kobayashi, H. Koch, K. V. Mikkelsen, P. Norman, M. J. Packer, T. Saue, P. R. Taylor, and O. Vahtras, *Dalton, an Ab Initio Electronic Structure Program, Release 1.0 (1997).* See http://www.kjemi.uio.no/software/dalton/dalton.html.
[23] J. G. Kirkwood and F. Westheimer, J. Chem. Phys. **6**, 506 (1936).
[24] K. V. Mikkelsen, E. Dalgaard, and P. Swanstrøm, J. Phys. Chem. **91**, 3081 (1987).
[25] K. V. Mikkelsen, H. Ågren, H. J. Aa. Jensen, and T. Helgaker, J. Chem. Phys. **89**, 3086 (1988).
[26] K. O. Sylvester-Hvid, K. V. Mikkelsen, and M. Ratner, J. Phys. Chem. (to be published).
[27] G. R. Alms, A. W. Burham, and W. H. Flygare, J. Chem. Phys. **63**, 3321 (1975).
[28] A. Proutiere and M. Camail, Mol. Phys. **29**, 1473 (1975).
[29] R. W. Hellwarth, Prog. Quantum Electron. **5**, 1 (1977).
[30] J. E. Bertie and Z. Lan, J. Chem. Phys. **103**, 10 152 (1995).